

Molecular Modeling and Simulations of Peptide–Polymer Conjugates

Phillip A. Taylor¹ and Arthi Jayaraman^{1,2}

¹Department of Chemical and Biomolecular Engineering, University of Delaware, Newark, Delaware 19716, USA; email: arthij@udel.edu

²Department of Materials Science and Engineering, University of Delaware, Newark, Delaware 19716, USA

Annu. Rev. Chem. Biomol. Eng. 2020. 11:257–76

The *Annual Review of Chemical and Biomolecular Engineering* is online at chembioeng.annualreviews.org

<https://doi.org/10.1146/annurev-chembioeng-092319-083243>

Copyright © 2020 by Annual Reviews.
All rights reserved

ANNUAL REVIEWS CONNECT

www.annualreviews.org

- Download figures
- Navigate cited references
- Keyword search
- Explore related articles
- Share via email or social media

Keywords

simulations, atomistic, coarse-grained, peptide–polymer conjugate

Abstract

Peptide–polymer conjugates are a class of soft materials composed of covalently linked blocks of protein/polypeptides and synthetic/natural polymers. These materials are practically useful in biological applications, such as drug delivery, DNA/gene delivery, and antimicrobial coatings, as well as nonbiological applications, such as electronics, separations, optics, and sensing. Given their broad applicability, there is motivation to understand the molecular and macroscale structure, dynamics, and thermodynamic behavior exhibited by such materials. We focus on the past and ongoing molecular simulation studies aimed at obtaining such fundamental understanding and predicting molecular design rules for the target function. We describe briefly the experimental work in this field that validates or motivates these computational studies. We also describe the various models (e.g., atomistic, coarse-grained, or hybrid) and simulation methods (e.g., stochastic versus deterministic, enhanced sampling) that have been used and the types of questions that have been answered using these computational approaches.

1. INTRODUCTION

Peptide–polymer conjugates are a complex class of biocompatible/bioderived/bioinspired soft materials (see 1–13 for review/perspective articles) that have gained significant attention from researchers in fields such as chemistry, materials science and engineering, biological science, and chemical engineering. From a practical standpoint, polymer conjugation imparts processability onto the peptides at conditions (i.e., solvent, temperature, pressure) that would not be possible with the protein/peptide alone, and the peptide imparts precision (e.g., sequence control and low dispersity) to the peptide–polymer conjugates that is not easy to program with synthetic polymers. Fundamentally, these peptide–polymer conjugates exhibit structural features on many length scales, from the monomer or amino acid contacts to the secondary and tertiary structures of the protein, polymer chain conformations, and domains formed from microphase separation of the polymer and protein/peptide in bulk/thin film or micelles formed from self-assembly in solutions of peptide–polymer conjugates. Along with structure, the thermodynamics is also complex; molecular-level thermodynamic driving forces for the protein/peptide to fold or aggregate can be altered by the attached polymer in a nonintuitive manner, motivating many fundamental studies to uncover these forces. Furthermore, the local (i.e., repeat unit) dynamics combined with dynamic macroscale (i.e., chains and domains) rearrangements at equilibrium and during processing is another nontrivial feature worth investigating. In addition to the exciting fundamental complexities that these macromolecules exhibit, materials composed of peptide–polymer conjugates find use in biological applications (14–21), such as drug delivery, protein therapeutics, gene delivery, and antimicrobial coatings, as well as nonbiological applications (22, 23), such as electronics, membrane separations, optics, and sensing (Figure 1).

Despite their many attractive fundamental and technological aspects (Figure 1a), few studies focus on peptide–polymer conjugates, compared to other synthetic and bio-derived

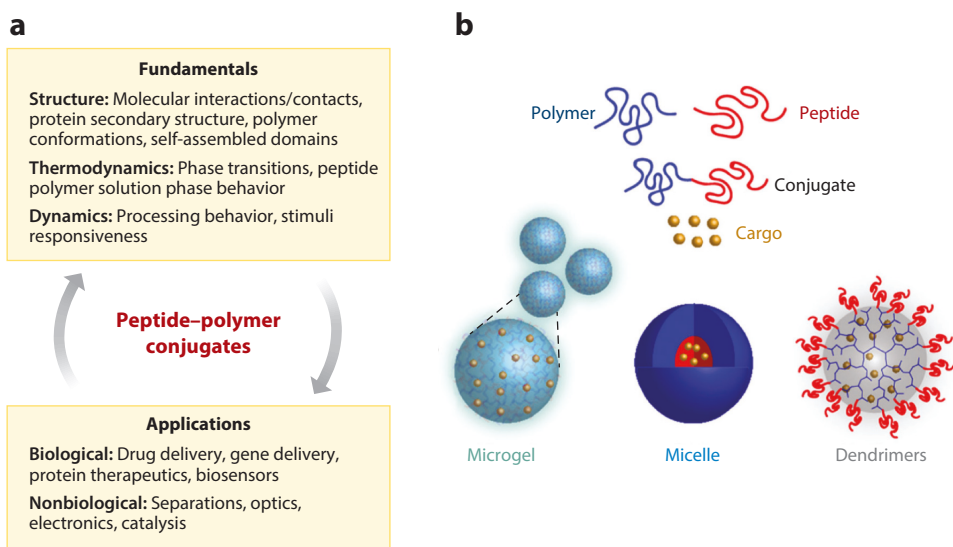


Figure 1

Peptide–polymer conjugates. (a) Fundamentals and applications, inspired by figure 1 in Reference 5. (b) Schematic of peptide–polymer conjugates and their self-assembly to form microgels, micelles, and dendrimers that can be loaded with cargo for delivery applications. Adapted from Reference 2 with permission from The Royal Society of Chemistry.

macromolecules (e.g., block copolymers, colloids, polysaccharides, proteins), because of the challenges they present in synthesis, characterization, and modeling (1, 5, 24, 25). Furthermore, the difficulties with purification lead to low yield despite high production cost and time. These challenges can hamper the speed with which one can design and optimize peptide–polymer conjugates for a specific application and thus motivate *in silico* studies to establish structure–function relationships for a variety of peptide–polymer candidates. Computational tools can also probe the impact of the polymer on the peptide/protein structure, dynamics, and function for varying polymer design, as well as elucidate how the peptide/protein impacts the polymer chain conformation.

Given this strong motivation for computational studies, we focus on past and ongoing modeling and simulation work on peptide–polymer conjugates. We first describe past experimental studies on peptide–polymer conjugates to identify the key fundamental questions and relevant length and timescales that these modeling and simulation studies should address. Then, we describe the types of models, simulation methods, and analysis techniques that have already been used or that have not been used yet but are appropriate for studying peptide–polymer conjugates.

Model:

a mathematical representation of the physical and chemical features of an atom or a group of atoms

Secondary structure:

an ordered structure of peptides/proteins stabilized by hydrophobic, electrostatic, and hydrogen bonding interactions

2. FUNDAMENTAL QUESTIONS POSED AND/OR PROBED BY EXPERIMENTS

Experimental studies on peptide–polymer conjugates, described in other review articles (2–13), have tried to answer these key fundamental questions: (a) What is the impact of polymer conjugation on peptide structure, thermal stability, and function? (b) What is the nanostructure when peptide–polymer conjugates self-assemble in solution, bulk, and thin films? (c) What are the thermodynamic driving forces for self-assembly, and what are the dynamics during self-assembly? It is expected that the structural stability of the peptide in the peptide–polymer conjugates will depend on polymer chemistry, molecular weight, peptide composition and sequence, the site on the peptide where the polymer is conjugated, and the solvent(s)/media. The architecture (linear, branched) and sequence (diblock, multiblock) of the polymer and the peptide combined together also play a critical role. One well-studied architecture and sequence is the linear diblock peptide–polymer conjugate, in which a linear polymer is conjugated to a peptide terminus (termed as end conjugated). The attached polymer, which is poly(ethylene glycol) (PEG) in many cases, has been shown to increasingly destabilize a peptide coil structure as the polymer length increases and/or peptide length decreases. This is partly because the monomer(s) near the attachment point on the peptide termini can be restricted in volume. Additionally, when multiple polymer chains are conjugated to the peptide, it causes crowding among the monomers of the attached polymer(s). This crowding among the monomers can be relieved by the unwinding/unfolding of the peptide secondary structure (10, 12). Going beyond the linear architecture, one can also conjugate polymer(s) as side chain(s) along the mid-section of the peptide’s secondary structure. To characterize the shape and size of these peptide–polymer conjugates, one can conduct small-angle X-ray and/or neutron scattering (24). Interpretation of the scattering results using analytical models like a Gaussian polymer chain attached to the middle section of a cylinder (for the peptide) has led to the conclusion that the side chain attachment of the polymer (PEG) in the peptide–polymer conjugate stabilizes the helical content of the peptide while adopting a compressed polymer conformation; this polymer conformation is more compressed compared to the same polymer either free in solution or in an end-conjugated architecture. Studies have found that the compressed configuration is due to an attractive interaction between the oxygen atoms of the PEG chain and the charged groups of the peptide (e.g., lysine, arginine, histidine).

The choice of the polymer chemistry plays a major role in the structure and function of the peptide in the peptide–polymer conjugate. PEG, owing to its biocompatible nature, has been the

most widely used in the peptide–polymer conjugate studies (16, 26–29), but many studies have used other polymer chemistries to achieve a specific function. For example, one could attach conducting polymers (e.g., polythiophene) to peptides to impart conductivity within bioelectronic materials (30). Another example is thermoresponsive polymers that alter their configurations/conformations in solution with temperature changes [e.g., poly(ethylene glycol methacrylate)]. Attaching such polymers to peptides could lead to new thermoresponsive properties in the peptide–polymer conjugates arising from the dual-phase transitions of the peptide and the polymer. Similarly, pH-responsive (31) or light-responsive polymers can also be synthesized and conjugated to the protein. Along the same lines, the solubility of the peptide–polymer conjugate can be altered by using hydrophilic versus hydrophobic polymer chemistry. In aqueous solutions, soluble peptides can be made to assemble into nanostructures through conjugation to a hydrophobic polymer. Even at the single chain level, depending on the peptide composition, sequence, and secondary structure, conjugating a hydrophobic polymer could impact the peptide structure and function. For example, in work by Shu et al. (32), upon conjugation of polystyrene to the N terminus of a heme-binding coiled-coil protein, owing to hydrophobic polymer-peptide interactions, the peptide secondary structure partially unfolded and, as a result, compromised the fidelity of the binding pocket within the core of the bundle. One common feature seen in many peptide–polymer conjugate systems in which the attached polymer destabilized the peptide was the presence of the amino acid residues at the polymer–peptide interfacial zone that lacked secondary structure (5). So, one design rule to consider for creating peptide–polymer conjugates while retaining protein structure and functionality is to select the architecture of the conjugate or the site of polymer conjugation that does not disrupt the interfacial-zone amino acids. Another design rule is the choice of the solvent rather than the polymer. For example, changing from aqueous to organic solvents that solubilize the hydrophobic polymers has been shown to enhance retention of the peptide structure. In such cases, the presence of the solvophilic polymers can stabilize the folded structures by shielding the protein from making unfavorable contacts with the solvent. Clearly, the interactions between the peptide, polymer, and solvent can be tailored, using molecular simulations, so as to dissolve the amphiphilic peptide–polymer conjugates, thus increasing solution processability while also retaining protein structure and function.

As stated briefly above, amphiphilicity (33) in peptide–polymer conjugates has been exploited for self-assembly in solutions to create precise (micelle-like) nanostructures (**Figure 1b**). Experiments have shown that micelles formed due to the amphiphilic nature of the peptide–polymer conjugates can be made to be stimuli-responsive through the choice of polymer chemistry. Furthermore, controlled changes in micelle structure can be brought about through changes in polymer conformation with varying solvent or temperature. For example, conjugation of a thermoresponsive triblock comprising poly(diethylene glycol methyl ether methacrylate) to the ends of a collagen-like peptide triple helix led to the formation of spherical aggregates that increased in size with increasing temperature up to 65°C and then transitioned to fibrils at 75°C (2, 34). Beyond solutions, both in bulk and in thin films (i.e., conditions in which the solvent composition in the eventual solid state/assembled state is minimal even though a prior solvent processing stage may have a large solvent content) peptide–polymer conjugates can also assemble into a variety of microphase-separated nanostructures like block copolymers do (35, 36) (e.g., hexagonal-in-zigzag lamellar, lamellae with liquid-crystalline arrangement in one domain, honeycomb arrangement within phase-separated domains). The balance between peptide–peptide interactions and polymer–peptide interactions is vital to controlling the thermodynamics of phase separation. The relative sizes and shapes of the peptides and polymers within each molecule dictate the shapes of the domains formed in solution/bulk as well as dynamics during the assembly.

The above experiments describe the relevant length scales of structural detail (polymer conformation, peptide secondary and/or tertiary structure, assembled domain sizes) and the balance of the various pair-wise interactions (polymer–peptide, peptide–solvent, polymer–solvent, peptide–peptide) that are important when choosing molecular models, simulation methods, and analysis. We describe next the types of models [e.g., atomistic versus coarse-grained (CG), or hybrid], simulation methods [e.g., Monte Carlo (MC) versus molecular dynamics (MD), unbiased versus biased sampling], and experimentally relevant computational analysis (e.g., free energy calculations, structure factors in inverse space, pair correlations in real space) that have been used in past studies or could potentially be used in future studies.

3. RELEVANT MOLECULAR MODEL AND SIMULATION METHODS FOR PEPTIDE–POLYMER CONJUGATES

Many review articles on macromolecular modeling and simulation methods (e.g., 25, 37–46) describe the advantages and disadvantages of the various molecular models one could use to simulate synthetic and biological macromolecules. Among macromolecular systems, peptide–polymer conjugates are unique (25) because they have a protein/polypeptide as one block, which typically requires chemically detailed models, and a synthetic polymer as another block, which has typically been studied successfully with CG models. Therefore, one must justify the use of a purely atomistic or purely CG model (and the level of coarse-graining) or a hybrid/multiscale model (44, 47). The following subsections describe the types of information that have been or can be obtained using simulations with atomistic, CG, or multi-scale models.

3.1. Atomistic Simulations

Atomistic simulations have been used extensively for studying peptides/proteins owing to their ability to capture salient features, such as peptides' secondary structures, peptide/protein unfolding transitions, and atom–atom contacts and interactions along the peptide chain (43, 48–50). These same reasons also make these atomistic approaches appropriate for peptide–polymer conjugates, especially if one wants to understand how polymer conjugation alters/stabilizes the peptide secondary structure. For example, Keten and coworkers (28) used an atomistic simulation of a coiled-coil peptide–PEG conjugate to show that the conjugation of three PEG chains to each helix did not induce helix unfolding but slightly enhanced the helical content of the conjugated peptides as compared to the nonconjugated coiled coil. They also observed that the radius of gyration (R_g) of isolated PEG chains versus three PEG chains conjugated to a helix was similar, indicating that a moderate conjugation density of three chains per helix was not high enough for the PEG chains to feel significant crowding effects. A snapshot of the atomistic coiled-coil peptide–PEG conjugate investigated by Keten and coworkers is shown in Figure 2a, along with a plot showing the effect of PEG conjugation and molecular weight (MW) on the helicity and dynamics of the peptides in the form of root mean squared displacement (RMSD). Other studies have shown that PEG can interact favorably with proteins, leading to a wrapped configuration of the peptide–polymer conjugate (28). Specifically, PEGylation has been shown to reduce the solvent-accessible surface area of peptides, stabilize protein secondary structures, and increase the conjugate's size—all of which can be correlated with an enhancement of circulation lifetimes and reduced immunogenicity, features critical for potential biological applications.

Although most atomistic studies have focused on PEG–peptide conjugates, other synthetic polymer chemistries have been conjugated to peptides either to drive formation of interesting assembled morphologies in solutions/melts or to impart electronic properties for engineering

Monte Carlo (MC) simulation: a broad class of stochastic simulations that rely on repeated random sampling to obtain ensemble averages

Structure factor: a mathematical description of how a material scatters incident radiation and gives details about the structure of a material

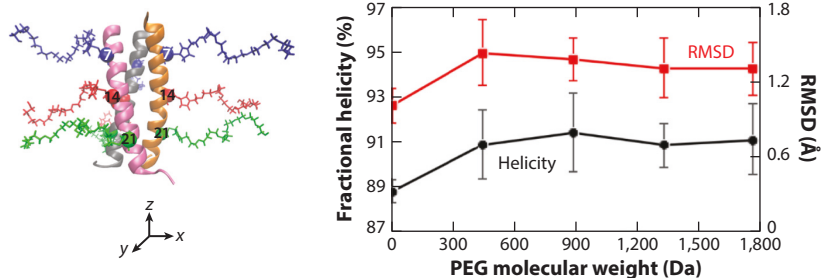
Coarse-graining: the process of reducing the degrees of freedom of a molecule by grouping atoms into lumped/coarse-grained beads

Coiled coil: a structural motif found in peptides in which 2–7 α -helices are coiled together in a ropelike fashion

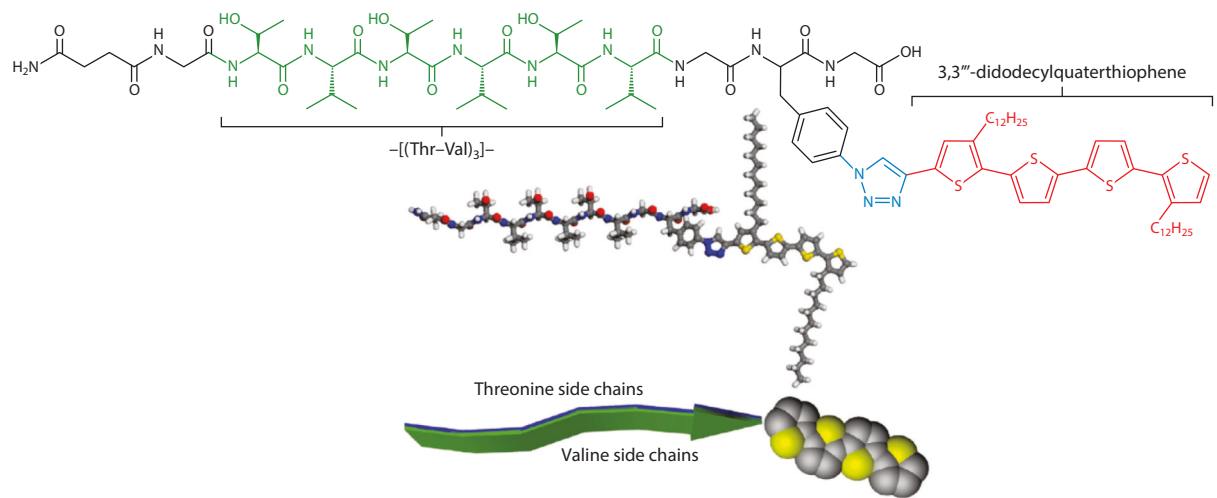
Radius of gyration (R_g): the average distance between any point on the molecule and its center of mass (i.e., the effective size of the molecule)

Root mean squared displacement (RMSD): a measure of the deviation of particle(s) with respect to a reference position over time

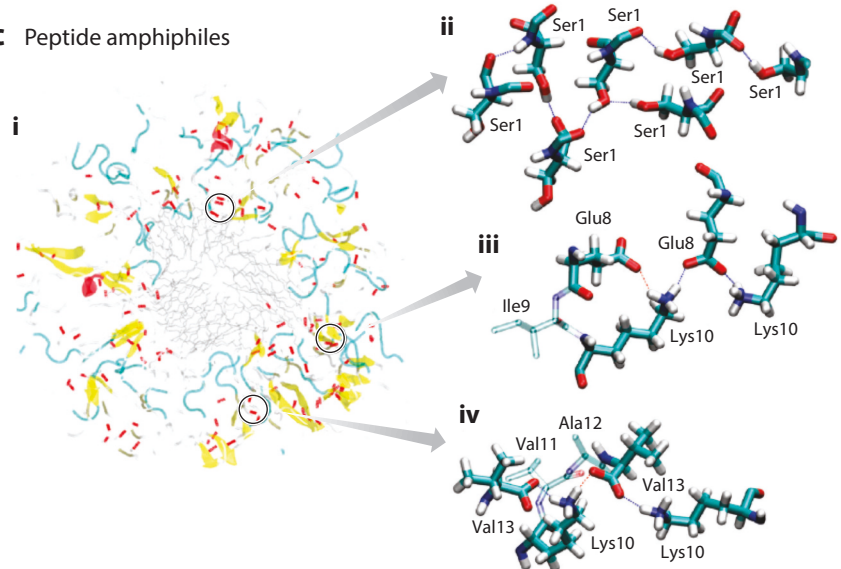
a Peptide–PEG conjugates



b Peptide–oligothiophene conjugates



c Peptide amphiphiles



(Caption appears on following page)

Figure 2 (Figure appears on preceding page)

Examples of atomistic simulation studies of peptide–polymer conjugates. (a) Schematic of an atomistic peptide–poly(ethylene glycol) (PEG) conjugate in which three PEG chains are attached to residues 7 (blue chains), 14 (red chains), and 21 (green chains) of each helix in a coiled coil (28). Also shown is a modified figure of the root mean squared displacement (RMSD) and fractional helicity obtained from Reference 28. Reprinted with permission from Reference 28; copyright 2015 American Chemical Society. (b) Different atomistic representations of the peptide–oligothiophene conjugates investigated by Khokhlov and coworkers (30). Reprinted with permission from Reference 30; copyright 2011 American Chemical Society. (c) Snapshot of the cross-section of the cylindrical nanofiber at 40 ns (56). All hydrogen bonds are illustrated using red lines, whereas peptide amphiphiles are displayed as transparent (left). Reprinted with permission from Reference 56; copyright 2011 American Chemical Society.

bioelectronic materials. For example, Alemán and coworkers (51) performed atomistic MD simulations of cyclic peptides conjugated to poly(*n*-butyl acrylate) (PnBA) and observed that both the unconjugated peptide and peptide–polymer conjugate preferably adopted an antiparallel conformation in solution in which lysine side chains formed favorable electrostatic interactions with glutamic acid side chains; the parallel conformation was disfavored owing to unfavorable electrostatic repulsion between neighboring charged moieties. Upon adsorption of the peptide–polymer conjugates to a mica surface, however, both the parallel and antiparallel conformations were stabilized by the formation of strong attractive interactions between the PnBA chains and the mica substrate. Peptides conjugated to oligo/polythiophenes, a class of conducting polymers, have also been studied using atomistic simulations. These peptide–polymer conjugates form microphase-separated morphologies driven by hydrophobicity, hydrogen bonding, and π – π stacking. In one study, Khokhlov and coworkers (52) performed atomistic MD simulations of an AB copolymer composed of α -tetrathiophene and a silk peptide segment (Gly-Ala-Gly-Ala-Gly) and an ABA copolymer containing a central α -tetrathiophene segment with two identical end blocks of peptide fragments, (Ala-Gly)₃. Using the polymer consistent force field (53–55), they showed that AB diblocks and ABA triblocks adsorbed to a layer of highly ordered pyrolytic graphene (HOPG), with the adsorbed surface density being dependent on the copolymer sequence. They also observed that for moderate adsorption strengths, both the diblock and triblock formed bilayers on the HOPG surface, stabilized by a network of hydrogen bonds between peptide blocks. For strong adsorption, however, the bilayer structure broke down and resulted in the formation of a system of 2D micelles. For diblocks, the micelles had a peptide core enveloped by thiophene segments; the β -sheet structure of the peptide remained intact. For triblocks, the bilayer structure broke down, and the planar micelles aggregated via the formation of new intermolecular hydrogen bonds. Khokhlov and coworkers (30) also studied polyethylene oxide–functionalized alkylated quaterthiophene– β -sheet peptide diblock oligomers (Figure 2b), which have been shown experimentally to self-assemble into fibrillar aggregates in organic solvent. They simulated both single- and double-layer β -sheets and constructed long fibrils via replication of the periodic cell along the axis of alignment. They observed that for single-layer fibrils with a parallel arrangement of β -strands composed of peptide–quaterthiophene conjugates, the fibril remained linear and axially rigid, unlike its all-peptide counterpart, which tended to collapse into a more compact structure.

Besides the above atomistic simulation studies focused on peptides conjugated with PEG and conducting polymers, there are also atomistic simulations on peptide amphiphile (PA) self-assembly driven by hydrophobic and electrostatic interactions. Schatz and coworkers (56) studied the relaxation of a self-assembled structure of 144 PA molecules into cylindrical nanofibers with explicitly represented water with a physiological ion concentration. By analyzing the nonbonded interaction energy, they concluded that the cylindrical fiber was stabilized by the electrostatic interactions between the PAs and the sodium ions, along with the van der Waals interactions between the PAs. They also found that the hydrogen bonding network was most prominent in the Ser-Leu-Ser-Leu region of the peptide, whereas salt bridges were formed between charged residues. Deng

Force field: the functional form used to describe the bonded and nonbonded interaction potentials of a system of atoms/coarse-grained particles

Initial configuration:
the initial positions
of all atoms/coarse-
grained particles in a
molecular simulation

and coworkers (57) also focused on the assembly of cylindrical nanofibers by β -sheet-forming PAs composed of four different fragments of the Alzheimer amyloid beta peptide, A β (residues 1 to 42), attached to a dodecanoyl hydrophobic tail (C12). They found that the capping of the peptide with a methyl amide group (NMA) impacted PA assembly. Specifically, they saw that mainly random coil structures were observed at pH 7 for end-capped systems, whereas β -sheet laminates were formed with increasing pH or via the removal of the capping ends. Furthermore, they observed that peptides with opposite charges on both sides of the peptide were found to have the fewest β -sheet structures in aggregates, whereas peptides with an isolated, single charged residue located at the center of the sequence were found to be able to promote the formation of regular β -sheets.

In all of the above atomistic simulation studies, the authors made some key decisions to obtain meaningful information from the simulation. The first was the choice of an appropriate force field(s) for the polymer, peptide, and solvent. For example, Alemán and coworkers (51) obtained interaction parameters (i.e., bonded and nonbonded potential forms and constants) for the amino acids contained in a cyclic peptide–PnBA conjugate from the AMBER ff03 force field, which has been shown to display good agreement with experiments in terms of structural and thermodynamic data for proteins and peptides (58). Then for the PnBA block in the peptide–polymer conjugate, they used the bonded and van der Waals parameters obtained from the generalized AMBER force field (59). For solvents, most peptide–polymer studies focused on aqueous systems use the TIP4P and TIP3P water models owing to their ability to accurately reproduce protein secondary structures (i.e., as a result of interactions between the peptide and water) as compared to simpler water models, such as the simple point charge (SPC) model (60). Another important decision when conducting atomistic simulations is the choice of an initial configuration. For most atomistic systems, large structural rearrangements are inaccessible owing to the limited sampling time that is possible with such systems, typically at most a few hundred nanoseconds. Therefore, most atomistic simulations involving large assemblies of peptide–polymer conjugates are preassembled into an initial configuration based on intuition or structural information from experiments. For example, as mentioned previously, Schatz and coworkers (56) simulated the self-assembly of 144 PAs into cylindrical nanofibers by initially placing 9 PAs radially on a plane with their tails pointing inward, as shown in **Figure 2c**. Then, a second layer was created along the fiber axis that was identical to the first layer but rotated relative to the first layer and with the distance between layers set at 5 Å. A total of 16 layers that alternated between the first and second layers were placed along the fiber axis to define the complete structure; the starting structure was chosen based on pilot simulations in which 9 molecules per layer was the highest density that led to a stable simulation without significant overlap between neighboring PAs. Another issue with atomistic systems is that they are limited in terms of system sizes. Although most atomistic studies of peptide–polymer conjugates involve multiple conjugates, with the goal of studying self-assembly, many of the box sizes used in such studies are limited to 10–50 nm.

To address some of the above limitations of atomistic simulations, researchers develop CG models that are better suited than atomistic models to study the self-assembly of large peptide–polymer systems from random initial configurations, to replicate large length and timescales relevant for experiments focused on the formation of the macro- or microstructures in solutions/melts of peptide–polymer conjugates.

3.2. Coarse-Grained Simulations

CG models reduce the degrees of freedom by representing groups of atoms as a collective CG bead, thus enabling computational speedup and simulations of larger systems at longer timescales. For peptide–polymer conjugates, with CG models one can simulate large systems (e.g., hundreds)

of peptide–polymers and predict self-assembly into ordered nanostructures from random initial configurations over timescales exceeding hundreds of nanoseconds. The first decision to make for these simulations is the type of CG model that is needed. One choice is generic CG models that have been used extensively to represent polymers [e.g., bead-spring models (61)]. Alternately, one may develop new CG models specifically for the system of interest using either (*a*) a bottom-up approach, in which the grouping of atoms into CG beads and their interactions are guided by/mapped from atomistic simulations, or (*b*) a top-down approach, in which the CG model is chosen to replicate experimental measurements or observations. There are also generalized models, such as MARTINI (62), which were originally developed for studying lipid bilayers and vesicles but in recent years have been extended to describe peptides/proteins and peptide–polymer conjugates (63, 64). MARTINI models use a four-to-one atom-to-CG bead mapping with approximately four heavy atoms and associated hydrogens mapped onto a single CG bead or interaction site. These CG beads are sorted into one of four types: polar, nonpolar, apolar, and charged. The MARTINI force field has been parameterized combining top-down and bottom-up approaches with the nonbonded interaction potentials based on experimental partitioning free energies between polar and apolar phases for a myriad of chemical compounds and the bonded interaction potentials derived from reference atomistic simulations. We direct the reader to Reference 63 which describes this MARTINI CG model development in detail. In a similar spirit, Go models (65) are generalized protein CG models, in which one CG bead represents one amino acid and simple attractive or repulsive nonbonded interactions between the CG beads are chosen to reproduce the intended folded protein secondary structure (66). We next describe a few example studies that have used these CG models or extended versions of the above CG models to tackle complex questions in peptide–polymer conjugates.

In one study, Keten and coworkers (28) developed a Go-like CG model of a coiled coil using the MMTSB Go Model Builder (67, 68), in which each residue is represented by a single bead located at the C α position of the corresponding amino acid. Using this Go-like model for the peptide with a generic bead-spring model for the polymer, they studied trimeric coiled coils conjugated with hydrophilic polymers (mimicking PEG). They showed that the conjugation site of the polymer, relative to the N or C terminus of the peptide, affected the conformation of the polymer chains and the overall thermal stability of the coiled coil. For side conjugation, each polymer chain formed a mushroomlike conformation around the exterior side of the helix, whereas for end conjugation the three polymer chains stayed in closer proximity as compared to the side-conjugated polymers. The helices with end-conjugated polymers had larger aggregation numbers and formed a smaller number of clusters as compared to side-conjugated polymers. In follow-up work, they used CG dissipative particle dynamics (DPD) simulations (69) to establish a simulation-driven design framework for controlling the size, shape, and stability of 3-helix micelles (**Figure 3a**). They studied coiled coils consisting of three α -helical peptides with each helical strand conjugated with an alkyl chain on the N terminus and a polymer chain located at various conjugation sites along each helical strand. Their simulations showed that smaller micelle size was achieved when polymers were attached closer to the hydrophobic peptide core. They created a phase diagram showing the packing parameter of the micelle as a function of conjugation position and degree of polymerization (DP). For low-DP polymers conjugated to the site nearest the alkyl core of the micelle, bilayer structures were observed. As the DP increased, spherical micelles were observed.

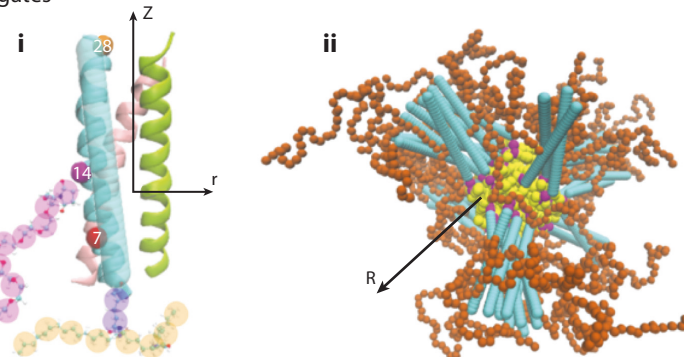
Similar to previous atomistic studies on peptide–polymer conjugates involving oligothiophenes, there have also been CG simulation studies on peptide-conducting polymer conjugates (70–72). Mansbach & Ferguson (70) developed a CG model of a peptide attached to oligophenylenevinylene (OPV) (**Figure 3b**), inspired by the MARTINI (63) model. For their CG model, the nonbonded interactions were adopted from the MARTINI force field, whereas bonded

Dissipative particle dynamics (DPD):
a mesoscale simulation method for complex fluids in which soft interaction potentials allow for enhanced sampling relative to traditional molecular dynamics

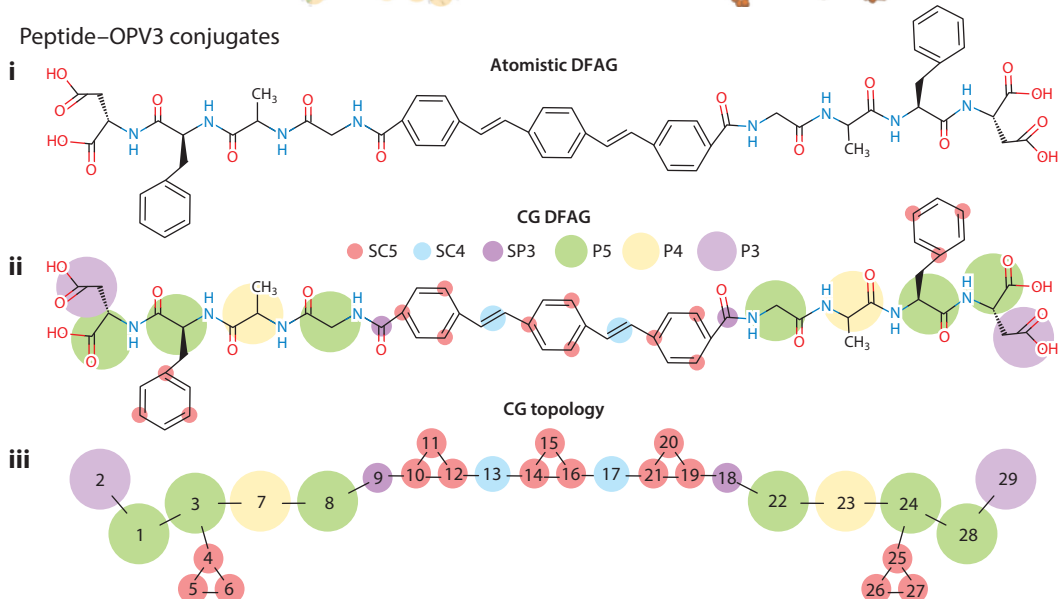
Packing parameter:
a metric that quantifies the geometric shape of a group of molecules (e.g., micelles)

Degree of polymerization (DP):
the number of monomers in a polymer chain

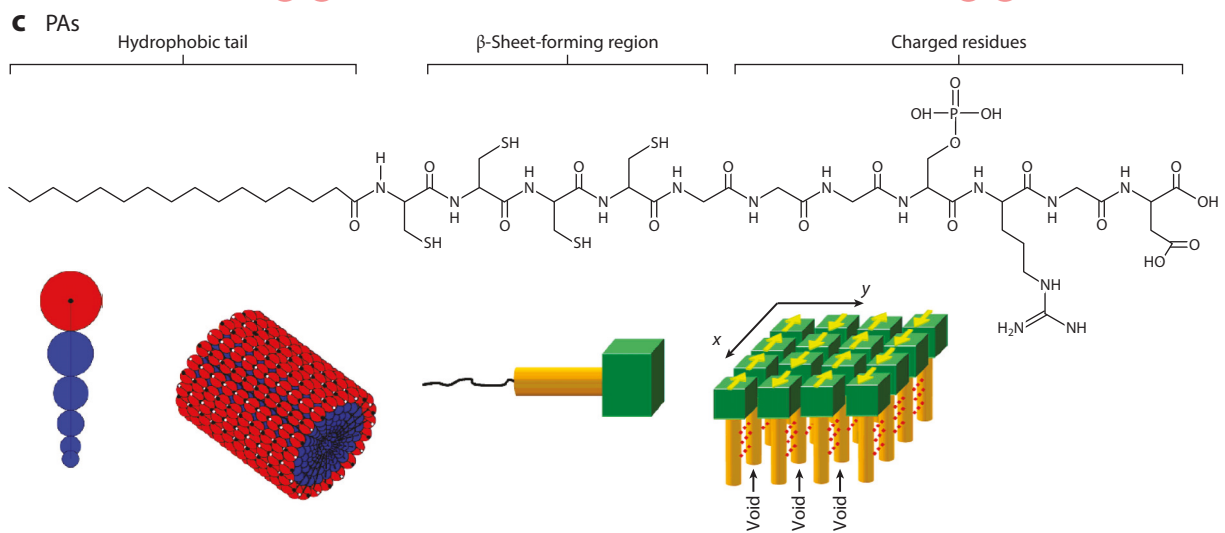
a Peptide–PEG conjugates



b Peptide–OPV3 conjugates



c PAs



(Caption appears on following page)

Figure 3 (Figure appears on preceding page)

Examples of coarse-grained (CG) simulation studies of peptide–polymer conjugates focused on self-assembly. (a, i) Schematic of a three-helix bundle investigated (69) with the poly(ethylene glycol) (PEG) chain and alkyl chain conjugated on one strand. (a, ii) A sample micelle with an aggregation number of 15, with PEG conjugated on residue 14 of the helix bundle. The helical strands (*cyan*) along with their conjugated PEG chains (*pink*) form the shell of the spherical micelle, whereas the alkyl chains (*yellow*) form the core of the micelle. Reproduced from Reference 69 with permission from The Royal Society of Chemistry. (b) Atomistic model of (Asp-Phe-Ala-Gly)-triphenylenevinylene-(Gly-Ala-Phe-Asp) or DFAG-OPV3-GAFD peptide–polymer conjugate investigated by Mansbach & Ferguson (70) and its corresponding CG representation mapped from the MARTINI model. Reprinted with permission from Reference 70; copyright 2017 American Chemical Society. (c) Self-assembly of a β -sheet-forming peptide amphiphile (PA) using the six-bead CG model, in which the bead sizes were chosen to mimic the cone shape of the atomistic structure of the PA, including electrostatic interactions (i.e., a dipole) in the head bead and hydrophobic interactions near the alkyl tail (74). Adapted with permission from Reference 74; copyright 2008 American Chemical Society.

parameters, such as bond stretching, angle bending, and proper and improper dihedrals, were extracted from 340-ns all-atom simulations using direct Boltzmann inversion (73). Their CG simulations showed that the potential of mean force (PMF) as a function of the peptide's end-to-end distance showed better agreement with the PMF obtained from all-atom simulations versus the original MARTINI model. Furthermore, they observed the formation of small optical and aligned clusters containing up to five conjugates. Two conjugates formed an optical cluster if the minimum distance between any beads in two aromatic rings was less than 0.7 nm, whereas aligned clusters refer to cases where all three aromatic rings of the OPV3 on a single conjugate are aligned with the three aromatic rings of the OPV3 of another conjugate and are therefore expected to exhibit the strongest electronic properties. Using such CG models, they could also establish the dynamics of the assembly, with the initial stages involving individual conjugates forming clusters of fewer than 8 conjugates with aligned aromatic cores, followed by their assembly into larger aggregates containing fewer than 40 conjugates exhibiting strong associations between π -conjugated cores. Follow-up work showed that similar π -conjugated systems exhibited different assembly rates and morphologies under different pH values and flow conditions (71). Furthermore, they concluded that increasing pH strongly affected the assembly kinetics of π -conjugated systems by disfavoring the formation of large aggregates owing to a partitioning of charged residues to the aggregate surface and an increase in surface charge density that scaled approximately linearly with cluster size and the fraction of charged monomers in the system. They also observed flow-induced alignment and ordering of aggregates to form elongated fibrils and fibers at time and length scales exceeding hundreds of nanoseconds and tens of nanometers.

Several CG simulation studies (74) also focus on the self-assembly of PAs (e.g., **Figure 3c**). Schatz and coworkers (75) studied the self-assembly of PAs into a cylindrical micelle starting from a homogeneous mixture of amphiphiles in aqueous solutions using a modified MARTINI model to include three representative secondary structures, such as sheets, turn structures, and random coils. For a standard MARTINI CG model, the secondary structure needs to be provided externally via the MARTINI force field and is maintained constant during the simulation. Schatz and coworkers observed that a mixed assortment of secondary structures, rather than a single type of structure, was needed to reproduce the multitude of structures observed in atomistic simulations. Moreover, they performed 9 independent 16- μ s simulation runs (such timescales are possible owing to coarse-graining) and observed spontaneous fiber formation in all cases. PA molecules first formed spherical micelles, followed by the formation of a 3D network of micelles via van der Waals interactions. Subsequently, as the hydrophobic core of the different micelles merged, the 3D network transformed into a fiber with a diameter of \sim 80 Å. Similarly, de la Cruz and coworkers (76) used a united atom CG model to investigate hydrophobic interactions between alkyl tails and the network of hydrogen bonds between peptide blocks on the self-assembly of PAs. For their CG

Potential of mean force (PMF): the free energy of a system as a function of reaction coordinate(s)

Enhanced sampling: a simulation technique whereby additional mathematical constraints are added to increase the number and/or types of configurations observed during a simulation

model, they included three kinds of beads: hydrophobic, peptide, and polar epitope beads. For PAs with purely hydrophobic interactions, monodisperse finite-sized micelles formed. For PAs with no hydrophobic effects but only hydrogen bonding, they observed step-by-step aggregation of molecules into 1D β -sheets.

Although the CG models highlighted above show the many advantages of coarse-graining, including the ability to simulate longer timescales (up to microseconds) and larger systems from random initial configurations, these models also have several limitations. The loss of chemical detail is an obvious drawback, but it is not always straightforward to determine *a priori* the relevant chemical details that are essential to capture the correct physics and the details that can be coarse-grained out. Also, as the work of Schatz and coworkers (75) highlighted, the incorporation of the correct protein secondary structure in a CG model is a nontrivial task. There are systems in which the correct distribution of secondary structures is not known *a priori* and can vary as a function of external conditions, such as temperature, pressure, salt concentration, and pH. For example, elastin-like peptides are known to undergo secondary structure formation/breaking with increasing temperature (77, 78), and traditional CG models such as MARTINI are unable to capture these structural transitions. Furthermore, a CG model that can capture accurate equilibrium structures and/or dynamics does not necessarily capture all physical properties. CG simulations are still limited in terms of timescales that are accessible, and workarounds involving preassembled structures (79) (e.g., preassembled collagen triple helices) are used to speed up the configurational and conformational sampling of the system. Another important issue to note is that as a result of coarse-graining, the ruggedness of the free energy landscape of the system is reduced. This artifact usually results in enhanced sampling owing to the presence of fewer energy barriers and leads to computational speedup in terms of differences between coarse-grained time and real simulation time. However, the ruggedness of the landscape may also be important because local minima can be missing, thus resulting in greater configurational sampling at the expense of missing intermediate states along the free energy landscape in which systems can become kinetically trapped.

3.3. Hybrid or Multi-Scale Simulations

To combine the best features of atomistic (Section 3.1) or CG (Section 3.2) models and to overcome their individual limitations, one could use hybrid models or methods in which a system is simultaneously/concurrently represented using both atomistic and CG models. Models with simultaneous/concurrent multi-length-scale representation (80) or adaptive resolution (41, 81–84) can be used to study the atomistic details of the protein (e.g., secondary structure, interactions within the protein) in the presence of the attached polymer and solvent without the excessive computational expense/time needed to simulate the entire system atomistically. In such adaptive resolution methods, the representation of one or more constituents of the system can change (or adapt) from atomistic to/from CG representation depending on their position with respect to the protein or to a specific point in the simulation box. For example, the solvent molecules alone could be treated in a hybrid manner, switching or adapting in resolution depending on their location from the center of mass of the protein/polymer or protein–polymer conjugate. Alternately, molecules/species (solvent, protein, and polymer) in regions near the protein and the protein–polymer conjugation point could be treated atomistically, and molecules farther from that zone could be treated in a CG manner to accomplish substantial speedups in computational time. Such hybrid resolution methods have been inspired by original quantum mechanics/molecular mechanics (QM/MM) approaches (85) in which the simulation was set up to treat one region quantum mechanically and a surrounding region classically. We direct the reader to a review article that describes such methods, both QM/MM and AA/CG, in the context of soft matter systems (41). Even

though such methods seem ideal, one must be aware of the many practical challenges the user will face when implementing such hybrid resolution models. For instance, it is important to treat the atomistic (AA), CG, and intermediate coupling or healing region in a thermodynamically consistent manner to avoid artificial (temperature or concentration) gradients and, depending on the ensemble, maintain the appropriate parameters constant. Another key challenge in such AA/CG adaptive resolution approaches is the reverse mapping of CG to AA resolution for molecules that move to the regions of interest from farther zones (42, 44, 86).

To the best of our knowledge, these hybrid/adaptive resolution approaches have not yet been applied to peptide/protein–polymer conjugates. However, several studies have tackled the changing resolution of the solvent (87) around the atomistically represented protein (88) or atomistically represented polymer chain (89). With such models and the state-of-the-art hardware and software, one could realistically simulate only one or two peptide/protein–polymer conjugate macromolecules in explicit solvent. However, even the results from such small-length scale hybrid model simulations can be valuable in the development of coarser models that can be used to simulate much larger systems. For example, to represent the solvent effects implicitly in coarser CG models, we need as input the knowledge of solvation around the protein and polymer, which may vary with the peptide and polymer design (chemical composition, molecular weight, architecture). An AA/CG hybrid resolution simulation can describe how solvation around the peptide/protein changes with variations in their design. An example of such a study is the work of Stanzione & Jayaraman (89) (**Figure 4a**), who calculated the solvation of the PEG chain as a function of the PEG architecture. Similarly, interactions between the polymer and peptide in the presence of solvent can be captured explicitly using these models and may inform the cross (peptide–polymer) interactions to use in implicit solvent and/or coarser models. For example, AA simulation studies of PEG polymer conjugated to DNA (not peptide/protein) revealed the interactions that the PEG chain has with the DNA and, in turn, informed the CG models of DNA–polymer conjugates on how these interactions should be incorporated as a function of solvent quality (90). Besides their use in the development of CG models, results from hybrid resolution simulations of a single peptide–polymer macromolecule could guide synthesis of the appropriate building block one desires to achieve target self-assembled structures.

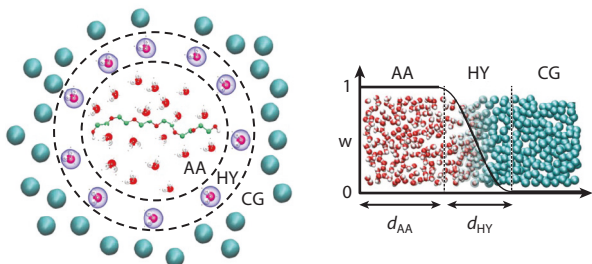
3.4. Advanced Simulation Methods

Most studies described in Sections 3.1–3.3 were done with standard MD simulations. One limitation of a standard MD simulation is the propensity for the system to become kinetically trapped in a local free energy minimum, thus reducing the sampling of other important configurations and/or conformations. To address this limitation of traditional/standard MD simulations especially, researchers have used stochastic simulations (e.g., MC, Brownian dynamics) and/or enhanced sampling techniques with MD simulations, such as steered MD (SMD) simulations (91), replica exchange (92), and metadynamics (93). Many of these methods have been applied to study peptides or polymers. For example, Theodorou and coworkers (94) developed novel moves within stochastic MC simulations to enhance configurational sampling of long chains of polyethylene (PE) (e.g., 500-mers or 1,000-mers) in melt-like conditions. Specifically, they developed MC moves—a double-bridging move and an intramolecular double-rebridging move that drastically change chain conformations in one move. They also showed that the computational efficiency of the two new MC moves remained unaltered with increasing molecular weight, in contrast to conventional MC moves or MD. Also, their simulations were able to predict the density of linear PE melts with varying molecular lengths within less than 1% of experimental measurements, and their structure factor calculations also showed agreement with experiments. Another example of

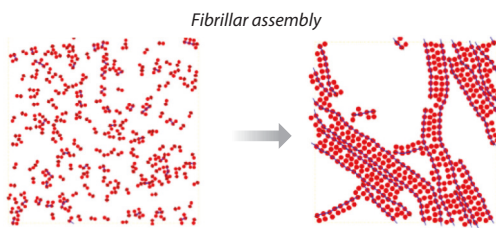
Brownian dynamics:
a stochastic simulation capturing the motion of particles in implicit solvent when viscous effects dominate over inertial effects

Steered molecular dynamics (SMD):
a molecular dynamics simulation in which an external force (not related to the force field) is applied to one or more atoms

a Adaptive/hybrid resolution simulations



b Monte Carlo simulations



c SMD simulations

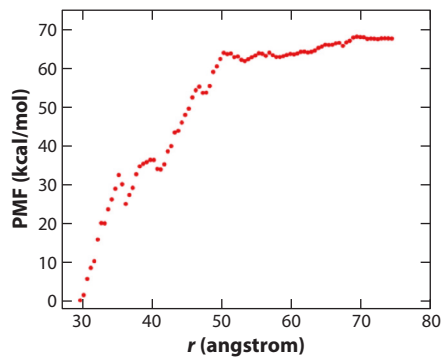
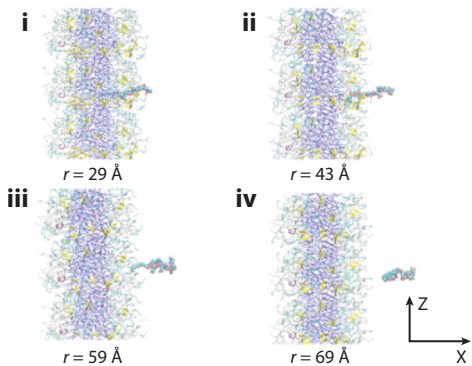


Figure 4

(a) Schematic representation of adaptive resolution model of a linear chain (in atomistic resolution) in water (adapting from atomistic to/from CG). The three regions in the simulation box are AA (*innermost sphere*), HY (*intermediate spherical shell*), and CG (*outermost shell*). Also shown is the positional implementation of this adaptive resolution method. Adapted with permission from Reference 89; copyright 2016 American Chemical Society. (b) Simulation snapshots show lack of peptide assembly at high temperatures and low densities and fibrillar assembly at low temperatures and high densities (95). Reprinted from Reference 95 with permission from Elsevier. (c) Representative snapshots taken from SMD simulations (96) of a PA being pulled out from a cylindrical micelle nanofiber at reaction coordinates, r , (i) $r = 29 \text{ \AA}$, (ii) $r = 43 \text{ \AA}$, (iii) $r = 59 \text{ \AA}$, and (iv) $r = 69 \text{ \AA}$. The reaction coordinate, r , is defined as the relative distance of the center of mass of the pulled PA with respect to the center of mass of the rest of the fiber. The potential of mean force shows that the free energy difference between a bound and free PA is -67 kcal/mol . Reprinted with permission from Reference 96; copyright 2013 American Chemical Society. Abbreviations: AA, atomistic; CG, coarse-grained; HY, hybrid; PA, peptide amphiphile; PEG, poly(ethylene glycol); PMF, potential of mean force; SMD, steered molecular dynamics.

MC simulation studies, by Urbic & Dias (95), reported the assembly of fibril-like structures made of amyloid proteins (**Figure 4b**). Using a CG model where a single peptide chain is modeled as 2D fused Lennard-Jones disks in which one disk represents the peptide backbone and another represents the peptide's side chains, they performed MC simulations of amyloid-like fibrils in two dimensions in the canonical (NVT) ensemble. They used three types of MC moves: translation, rotation, and switching (i.e., a rotation of 180°) for each peptide chain. They observed that at low densities and high temperatures, molecules were mostly present as individual peptide chains, whereas at low temperatures and higher densities, fibrils formed and subsequently associated to form higher-order structures composed of stacks of fibrils. These types of MC approaches could be applied to assembly of peptide–polymer conjugates as well.

Many peptide and polymer studies have used SMD to calculate the PMF of two macromolecules as a function of their intermolecular distance. To that end, Schatz and coworkers (96)

studied the self-assembly of PAs into cylindrical micelles using SMD based on a simple model that considered the aggregation of a single PA and a fiber composed of the same PAs to produce a fiber with one additional PA (**Figure 4c**). Following up on their previous work on the self-assembly of an atomistic Ser-Leu-Ser-Leu containing PA (56), they initially constructed circular disks of PAs to seed the cylindrical micelle structure. Next, using SMD simulations, the center of mass of a single PA was pulled, and the other 89 PAs in the nanofiber were constrained by applying a harmonic force at the last carbon of the hydrophobic tail of each PA. Then, the free energy as a function of the distance between the centers of mass of the pulled PA and the nanofiber was computed using Jarzynski's equality, in which the change in free energy is related to the external nonequilibrium work done by the pulling force during the SMD simulation. Their PMF calculations showed that the driving force for PA assembly was enthalpic, with both electrostatic and van der Waals interactions playing prominent roles. They observed that as the PA was pulled from the fiber, the interactions evolved through three stages: (a) Initially electrostatic interactions between the charged head of the pulled PA and PAs in the fiber, and between the solvent and PA, were dominant; (b) after the charged head emerged from the fiber and the rest of the peptide came out, both PA-solvent electrostatic interactions and van der Waals interactions became significant; and (c) as the alkane tail emerged, van der Waals interactions with either the peptide or alkane became dominant. In a similar study, Keten and coworkers (97) also used SMD to study how α -helices unfold under contact mechanical stress, and they determined that PEGylation was an effective strategy for reinforcing small helical proteins against mechanical stress. They studied a single helical strand of a 3-helix coiled coil, which was side conjugated (i.e., at residue 14) with a PEG chain containing 40 PEG monomers. By applying harmonic forces at both termini in the direction of the helix axis, they assessed helix stability under mechanical loading for constant tensile forces ranging from 52 to 695 pN. They observed that the helix unfolding time was greater for PEGylated peptides compared to native helices. They also concluded that the unfolding of a protein can be viewed as a sequence of events, including unfolding bursts, refolding, and plateau periods corresponding to periods with marginal structural rearrangements. These studies show that moving toward advanced (equilibrium and nonequilibrium) simulation methods beyond standard MD can be powerful in terms of the information gained about both the design and processing of peptide–polymer conjugates.

4. CONCLUSIONS

In this review, we have highlighted from the literature many examples of computational studies focused on peptide–polymer or protein–polymer conjugates. These examples were chosen to illustrate the types of molecular models—atomistic, CG, and hybrid—and simulation methods—MD, MC, DPD, and SMD—that have been used to answer a broad range of questions posed by experimental studies on these systems. These questions were outlined in the beginning of this review through a brief overview of key experimental studies. We have also described the main challenges and limitations in experiments that motivate the computational investigations. The cited computational studies demonstrate how molecular modeling and simulations can provide (a) an understanding of the impact of polymer conjugation on peptide/protein structure, thermal stability, and function; (b) a description of the overall shape/size and amphiphilicity of the polymer–peptide conjugates and their assembly characteristics; and (c) design rules (e.g., site of conjugation on the peptide and the number of polymer chains conjugated to the peptide) to achieve the desired peptide–polymer building blocks for target applications (e.g., drug delivery, bioelectronics, etc.). One important and promising direction for future studies is the use of computations for specifically probing dynamics in peptide–polymer conjugate systems. We have also shown how

the choice of the appropriate model and simulation method is strongly dependent on the question one wishes to answer, as well as the experimentally relevant length and timescales. With the advances in computer hardware, software, and new synthesis techniques, one should be able to harness the growing power of molecular modeling and simulations to further understand and design novel peptide–polymer conjugates.

DISCLOSURE STATEMENT

The authors are not aware of any affiliations, memberships, funding, or financial holdings that might be perceived as affecting the objectivity of this review.

ACKNOWLEDGMENTS

The authors are grateful for financial support from the National Science Foundation CBET (Chemical, Bioengineering, Environmental, and Transport Systems) 1703402 during the course of this manuscript preparation.

LITERATURE CITED

1. Russell AJ, Baker SL, Colina CM, Figg CA, Kaar JL, et al. 2018. Next generation protein–polymer conjugates. *AIChE J.* 64:3230–45
2. Paik BA, Mane SR, Jia XQ, Kiick KL. 2017. Responsive hybrid (poly)peptide–polymer conjugates. *J. Mater. Chem. B* 5:8274–88
3. Trzebicka B, Szweda R, Kosowski D, Szweda D, Otułakowski L, et al. 2017. Thermoresponsive polymer–peptide/protein conjugates. *Progress Polymer Sci.* 68:35–76
4. Pelegri-O'Day EM, Lin E-W, Maynard HD. 2014. Therapeutic protein–polymer conjugates: advancing beyond PEGylation. *J. Am. Chem. Soc.* 136:14323–32
5. Shu JY, Panganiban B, Xu T. 2013. Peptide–polymer conjugates: from fundamental science to application. *Annu. Rev. Phys. Chem.* 64:631–57
6. Dehn S, Chapman R, Jolliffe KA, Perrier S. 2011. Synthetic strategies for the design of peptide/polymer conjugates. *Polymer Rev.* 51:214–34
7. Borner HG. 2011. Precision polymers—modern tools to understand and program macromolecular interactions. *Macromol. Rapid Commun.* 32:115–26
8. Rabotyagova OS, Cebe P, Kaplan DL. 2011. Protein-based block copolymers. *Biomacromolecules* 12:269–89
9. Grover GN, Maynard HD. 2010. Protein–polymer conjugates: synthetic approaches by controlled radical polymerizations and interesting applications. *Curr. Opin. Chem. Biol.* 14:818–27
10. Klok HA. 2009. Peptide/protein-synthetic polymer conjugates: *quo vadis*. *Macromolecules* 42:7990–8000
11. Robson Marsden H, Kros A. 2009. Polymer–peptide block copolymers—an overview and assessment of synthesis methods. *Macromol. Biosci.* 9:939–51
12. Gauthier MA, Klok HA. 2008. Peptide/protein–polymer conjugates: synthetic strategies and design concepts. *Chem. Commun.* 23:2591–611
13. Hoffman AS, Stayton PS. 2007. Conjugates of stimuli-responsive polymers and proteins. *Progress Polymer Sci.* 32:922–32
14. Castelletto V, Kendrick JE, Hamley IW, Olsson U, Cenker C. 2010. PEGylated amyloid peptide nanocontainer delivery and release system. *Langmuir* 26:11624–27
15. Ang J, Ma D, Lund R, Keten S, Xu T. 2016. Internal structure of 15 nm 3-helix micelle revealed by small-angle neutron scattering and coarse-grained MD simulation. *Biomacromolecules* 17:3262–67
16. Dong H, Dube N, Shu JY, Seo JW, Mahakian LM, et al. 2012. Long-circulating 15 nm micelles based on amphiphilic 3-helix peptide-PEG conjugates. *ACS Nano* 6:5320–29

17. Dube N, Seo JW, Dong H, Shu JY, Lund R, et al. 2014. Effect of alkyl length of peptide–polymer amphiphile on cargo encapsulation stability and pharmacokinetics of 3-helix micelles. *Biomacromolecules* 15:2963–70
18. Sun H, Hong YX, Xi YJ, Zou YJ, Gao JY, Du JZ. 2018. Synthesis, self-assembly, and biomedical applications of antimicrobial peptide–polymer conjugates. *Biomacromolecules* 19:1701–20
19. ten Cate MGJ, Borner HG. 2007. Synthesis of ABC-triblock peptide–polymer conjugates for the positioning of peptide segments within block copolymer aggregates. *Macromol. Chem. Phys.* 208:1437–46
20. Kukula H, Schlaad H, Antonietti M, Förster S. 2002. The formation of polymer vesicles or “peptosomes” by polybutadiene-*block*-poly(L-glutamate)s in dilute aqueous solution. *J. Am. Chem. Soc.* 124:1658–63
21. Kumar P, Takayesu A, Abbasi U, Kalathottukaren MT, Abbina S, et al. 2017. Antimicrobial peptide–polymer conjugates with high activity: influence of polymer molecular weight and peptide sequence on antimicrobial activity, proteolysis, and biocompatibility. *ACS Appl. Mater. Interfaces* 9:37575–86
22. Ho D, Chu B, Schmidt JJ, Brooks EK, Montemagno CD. 2004. Hybrid protein–polymer biomimetic membranes. *IEEE Trans. Nanotechnol.* 3:256–63
23. Ayyagari MS, Pande R, Kamtekar S, Gao H, Marx KA, et al. 1995. Molecular assembly of proteins and conjugated polymers—toward development of biosensors. *Biotechnol. Bioeng.* 45:116–21
24. Pokorski JK, Hore MJA. 2019. Structural characterization of protein–polymer conjugates for biomedical applications with small-angle scattering. *Curr. Opin. Colloid Interface Sci.* 42:157–68
25. Lin P, Colina CM. 2019. Molecular simulation of protein–polymer conjugates. *Curr. Opin. Chem. Eng.* 23:44–50
26. Jain A, Ashbaugh HS. 2011. Helix stabilization of poly(ethylene glycol)–peptide conjugates. *Biomacromolecules* 12:2729–34
27. Hamed E, Xu T, Keten S. 2013. Poly(ethylene glycol) conjugation stabilizes the secondary structure of α -helices by reducing peptide solvent accessible surface area. *Biomacromolecules* 14:4053–60
28. Hamed E, Ma D, Keten S. 2015. Multiple PEG chains attached onto the surface of a helix bundle: conformations and implications. *ACS Biomater. Sci. Eng.* 1:79–84
29. Sousa SF, Peres J, Coelho M, Vieira TF. 2018. Analyzing PEGylation through molecular dynamics simulations. *ChemistrySelect* 3:8415–27
30. Shaytan AK, Schillinger E-K, Khalatur PG, Mena-Osteritz E, Hentschel J, et al. 2011. Self-assembling nanofibers from thiophene–peptide diblock oligomers: a combined experimental and computer simulations study. *ACS Nano* 5:6894–909
31. Catrouillet S, Brendel JC, Larnaudie S, Barlow T, Jolliffe KA, Perrier S. 2016. Tunable length of cyclic peptide–polymer conjugate self-assemblies in water. *ACS Macro Lett.* 5:1119–23
32. Shu JY, Huang Y-J, Tan C, Presley AD, Chang J, Xu T. 2010. Amphiphilic peptide–polymer conjugates based on the coiled-coil helix bundle. *Biomacromolecules* 11:1443–52
33. Hannink JM, Cornelissen JJLM, Farrera JA, Foubert P, De Schryver FC, et al. 2001. Protein–polymer hybrid amphiphiles. *Angew. Chem. Int. Ed.* 40:4732–34
34. Luo TZ, Kiick KL. 2013. Collagen-like peptides and peptide–polymer conjugates in the design of assembled materials. *Eur. Polymer J.* 49:2998–3009
35. Suguri T, Olsen BD. 2019. Topology effects on protein–polymer block copolymer self-assembly. *Polymer Chem.* 10:1751–61
36. Lam CN, Chang D, Wang M, Chen W-R, Olsen BD. 2016. The shape of protein–polymer conjugates in dilute solution. *J. Polymer Sci. A* 54:292–302
37. Gartner TE, Jayaraman A. 2019. Modeling and simulations of polymers: a roadmap. *Macromolecules* 52:755–86
38. Gooneie A, Schuschnigg S, Holzer C. 2017. A review of multiscale computational methods in polymeric materials. *Polymers* 9:16
39. Brini E, Algaer EA, Ganguly P, Li C, Rodríguez-Ropero F, van der Vegt NFA. 2013. Systematic coarse-graining methods for soft matter simulations—a review. *Soft Matter* 9:2108–19
40. de Pablo JJ. 2011. Coarse-grained simulations of macromolecules: from DNA to nanocomposites. *Annu. Rev. Phys. Chem.* 62:555–74
41. Nielsen SO, Bulo RE, Moore PB, Ensing B. 2010. Recent progress in adaptive multiscale molecular dynamics simulations of soft matter. *Phys. Chem. Chem. Phys.* 12:12401–14

42. Peter C, Kremer K. 2009. Multiscale simulation of soft matter systems—from the atomistic to the coarse-grained level and back. *Soft Matter* 5:4357–66
43. Zhou HX. 2004. Polymer models of protein stability, folding, and interactions. *Biochemistry* 43:2141–54
44. Müller-Plathe F. 2002. Coarse-graining in polymer simulation: from the atomistic to the mesoscopic scale and back. *ChemPhysChem* 3:754–69
45. Baschnagel J, Binder K, Doruker P, Gusev AA, Hahn O, et al. 2000. Bridging the gap between atomistic and coarse-grained models of polymers: status and perspectives. In *Advances in Polymer Science*, Vol. 152: *Viscoelasticity, Atomistic Models, Statistical Chemistry*, ed. A Abe, pp. 41–156. Berlin: Springer-Verlag
46. Binder K, Paul W. 1997. Monte Carlo simulations of polymer dynamics: recent advances. *J. Polymer Sci. B* 35:1–31
47. Peter C, Kremer K. 2010. Multiscale simulation of soft matter systems. *Faraday Discuss.* 144:9–24
48. Dill KA, MacCallum JL. 2012. The protein-folding problem, 50 years on. *Science* 338:1042–46
49. Childers MC, Daggett V. 2017. Insights from molecular dynamics simulations for computational protein design. *Mol. Syst. Des. Eng.* 2:9–33
50. Carballo-Pacheco M, Strodel B. 2016. Advances in the simulation of protein aggregation at the atomistic scale. *J. Phys. Chem. B* 120:2991–99
51. Bertran O, Curcó D, Zanuy D, Alemán C. 2013. Atomistic organization and characterization of tube-like assemblies comprising peptide–polymer conjugates: computer simulation studies. *Faraday Discuss.* 166:59–82
52. Gus'kova O, Schillinger E, Khalatur P, Bäuerle P, Khokhlov A. 2009. Bioinspired hybrid systems based on oligothiophenes and peptides (ALA-GLY)_n: computer-aided simulation of adsorption layers. *J. Polymer Sci. A* 51:430–45
53. Hwang M, Stockfisch T, Hagler A. 1994. Derivation of class II force fields. 2. Derivation and characterization of a class II force field, CFF93, for the alkyl functional group and alkane molecules. *J. Am. Chem. Soc.* 116:2515–25
54. Peng Z, Ewig CS, Hwang M-J, Waldman M, Hagler AT. 1997. Derivation of class II force fields. 4. Van der Waals parameters of Alkali metal cations and halide anions. *J. Phys. Chem. A* 101:7243–52
55. Sun H. 1994. Force field for computation of conformational energies, structures, and vibrational frequencies of aromatic polyesters. *J. Comput. Chem.* 15:752–68
56. Lee OS, Stupp SI, Schatz GC. 2011. Atomistic molecular dynamics simulations of peptide amphiphile self-assembly into cylindrical nanofibers. *J. Am. Chem. Soc.* 133:3677–83
57. Wu R, Liu J, Qiu X, Deng M. 2017. Molecular dynamics simulation of the nanofibrils formed by amyloid-based peptide amphiphiles. *Mol. Simul.* 43:1227–39
58. Duan Y, Wu C, Chowdhury S, Lee MC, Xiong G, et al. 2003. A point-charge force field for molecular mechanics simulations of proteins based on condensed-phase quantum mechanical calculations. *J. Comput. Chem.* 24:1999–2012
59. Wang J, Wolf RM, Caldwell JW, Kollman PA, Case DA. 2004. Development and testing of a general amber force field. *J. Comput. Chem.* 25:1157–74
60. Ksenofontova O. 2014. Investigation of conformational mobility of insulin superfamily peptides: use of SPC/E and TIP4P water models. *Mol. Biol.* 48:432–38
61. Kremer K, Grest GS. 1990. Dynamics of entangled linear polymer melts: a molecular-dynamics simulation. *J. Chem. Phys.* 92:5057–86
62. Marrink SJ, Risselada HJ, Yefimov S, Tieleman DP, de Vries AH. 2007. The MARTINI force field: coarse grained model for biomolecular simulations. *J. Phys. Chem. B* 111:7812–24
63. Monticelli L, Kandasamy SK, Periole X, Larson RG, Tieleman DP, Marrink S-J. 2008. The MARTINI coarse-grained force field: extension to proteins. *J. Chem. Theory Comput.* 4:819–34
64. Ramezanghorbani F, Lin P, Colina CM. 2018. Optimizing protein–polymer interactions in a poly(ethylene glycol) coarse-grained model. *J. Phys. Chem. B* 122:7997–8005
65. Ueda Y, Taketomi H, Gō N. 1978. Studies on protein folding, unfolding, and fluctuations by computer simulation. II. A. Three-dimensional lattice model of lysozyme. *Biopolymers Orig. Res. Biomol.* 17:1531–48
66. Tozzini V. 2005. Coarse-grained models for proteins. *Curr. Opin. Struct. Biol.* 15:144–50
67. Karanicolas J, Brooks CL III. 2002. The origins of asymmetry in the folding transition states of protein L and protein G. *Protein Sci.* 11:2351–61

68. Karanicolas J, Brooks CL III. 2003. Improved Gō-like models demonstrate the robustness of protein folding mechanisms towards non-native interactions. *J. Mol. Biol.* 334:309–25
69. Ma D, DeBenedictis EP, Lund R, Keten S. 2016. Design of polymer conjugated 3-helix micelles as nanocarriers with tunable shapes. *Nanoscale* 8:19334–42
70. Mansbach RA, Ferguson AL. 2017. Coarse-grained molecular simulation of the hierarchical self-assembly of π -conjugated optoelectronic peptides. *J. Phys. Chem. B* 121:1684–706
71. Mansbach RA, Ferguson AL. 2017. Control of the hierarchical assembly of π -conjugated optoelectronic peptides by pH and flow. *Org. Biomol. Chem.* 15:5484–502
72. Mansbach RA, Ferguson AL. 2018. Patchy particle model of the hierarchical self-assembly of π -conjugated optoelectronic peptides. *J. Phys. Chem. B* 122:10219–36
73. Noid WG. 2013. Perspective: coarse-grained models for biomolecular systems. *J. Chem. Phys.* 139:090901
74. McCullagh M, Prytkova T, Tonzani S, Winter ND, Schatz GC. 2008. Modeling self-assembly processes driven by nonbonded interactions in soft materials. *J. Phys. Chem. B* 112:10388–98
75. Lee OS, Cho V, Schatz GC. 2012. Modeling the self-assembly of peptide amphiphiles into fibers using coarse-grained molecular dynamics. *Nano Lett.* 129:4907–13
76. Velichko YS, Stupp SI, de la Cruz MO. 2008. Molecular simulation study of peptide amphiphile self-assembly. *J. Phys. Chem. B* 112:2326–34
77. Nuhn H, Klok H-A. 2008. Secondary structure formation and LCST behavior of short elastin-like peptides. *Biomacromolecules* 9:2755–63
78. Prashanna A, Taylor PA, Qin J, Kück KL, Jayaraman A. 2019. Effect of peptide sequence on the LCST-like transition of elastin-like peptides and elastin-like peptide–collagen-like peptide conjugates: simulations and experiments. *Biomacromolecules* 20:1178–89
79. Condon JE, Jayaraman A. 2018. Development of a coarse-grained model of collagen-like peptide (CLP) for studies of CLP triple helix melting. *J. Phys. Chem. B* 122:1929–39
80. Renevey A, Riniker S. 2017. Improved accuracy of hybrid atomistic/coarse-grained simulations using reparametrised interactions. *J. Chem. Phys.* 146:124131
81. Praprotnik M, Site LD, Kremer K. 2005. Adaptive resolution molecular-dynamics simulation: changing the degrees of freedom on the fly. *J. Chem. Phys.* 123:224106
82. Ensing B, Nielsen SO, Moore PB, Klein ML, Parrinello M. 2007. Energy conservation in adaptive hybrid atomistic/coarse-grain molecular dynamics. *J. Chem. Theory Comput.* 3:1100–5
83. Wang H, Schütte C, Delle Site L. 2012. Adaptive resolution simulation (AdResS): a smooth thermodynamic and structural transition from atomistic to coarse grained resolution and vice versa in a grand canonical fashion. *J. Chem. Theory Comput.* 8:2878–87
84. Zavadlav J, Praprotnik M. 2017. Adaptive resolution simulations coupling atomistic water to dissipative particle dynamics. *J. Chem. Phys.* 147:114110
85. Warshel A, Levitt M. 1976. Theoretical studies of enzymic reactions: dielectric, electrostatic and steric stabilization of the carbonium ion in the reaction of lysozyme. *J. Mol. Biol.* 103:227–49
86. Krajniak J, Pandiyan S, Nies E, Samaey G. 2016. Generic adaptive resolution method for reverse mapping of polymers from coarse-grained to atomistic descriptions. *J. Chem. Theory Comput.* 12:5549–62
87. Kuhn AB, Gopal SM, Schafer LV. 2015. On using atomistic solvent layers in hybrid all-atom/coarse-grained molecular dynamics simulations. *J. Chem. Theory Comput.* 11:4460–72
88. Zavadlav J, Nuno Melo M, Marrink S, Praprotnik M. 2014. Adaptive resolution simulation of an atomistic protein in MARTINI water. *J. Chem. Phys.* 140:054114
89. Stanzione F, Jayaraman A. 2016. Hybrid atomistic and coarse-grained molecular dynamics simulations of polyethylene glycol (PEG) in explicit water. *J. Phys. Chem. B* 120:4160–73
90. Ghobadi AF, Jayaraman A. 2016. Effects of polymer conjugation on hybridization thermodynamics of oligonucleic acids. *J. Phys. Chem. B* 120:9788–99
91. Leech J, Prins JF, Hermans J. 1996. SMD: visual steering of molecular dynamics for protein design. *IEEE Comput. Sci.* 3:38–45
92. Hukushima K, Nemoto K. 1996. Exchange Monte Carlo method and application to spin glass simulations. *J. Phys. Soc. Jpn.* 65:1604–8
93. Laio A, Parrinello M. 2002. Escaping free-energy minima. *PNAS* 99:12562–66

94. Karayiannis NC, Mavrntzas VG, Theodorou DN. 2002. A novel Monte Carlo scheme for the rapid equilibration of atomistic model polymer systems of precisely defined molecular architecture. *Phys. Rev. Lett.* 88:105503
95. Urbic T, Dias CL. 2019. Thermodynamic properties of amyloid fibrils: a simple model of peptide aggregation. *Fluid Phase Equilib.* 489:104–10
96. Yu T, Lee OS, Schatz GC. 2013. Steered molecular dynamics studies of the potential of mean force for peptide amphiphile self-assembly into cylindrical nanofibers. *J. Phys. Chem. A* 117:7453–60
97. Debenedictis EP, Hamed E, Keten S. 2016. Mechanical reinforcement of proteins with polymer conjugation. *ACS Nano* 10:2259–67



Annual Review of
Chemical and
Biomolecular
Engineering

Volume 11, 2020

Contents

A ChemE Grows in Brooklyn <i>Carol K. Hall</i>	1
Life and Times in Engineering and Chemical Engineering <i>J.F. Davidson</i>	23
Biological Assembly of Modular Protein Building Blocks as Sensing, Delivery, and Therapeutic Agents <i>Emily A. Berckman, Emily J. Hartzell, Alexander A. Mitkas, Qing Sun, and Wilfred Chen</i>	35
Bioprivileged Molecules: Integrating Biological and Chemical Catalysis for Biomass Conversion <i>Jiajie Huo and Brent H. Shanks</i>	63
Cellular Automata in Chemistry and Chemical Engineering <i>Natalia V. Menshutina, Andrey V. Kolnoochenko, and Evgeniy A. Lebedev</i>	87
Computational Fluid Dynamics for Fixed Bed Reactor Design <i>Anthony G. Dixon and Behnam Partopour</i>	109
Covalent Organic Frameworks in Separation <i>Saikat Das, Jie Feng, and Wei Wang</i>	131
How Do Cells Adapt? Stories Told in Landscapes <i>Luca Agozzino, Gábor Balázsi, Jin Wang, and Ken A. Dill</i>	155
Hydrolysis and Solvolysis as Benign Routes for the End-of-Life Management of Thermoset Polymer Waste <i>Minjie Shen, Hongda Cao, and Megan L. Robertson</i>	183
Life Cycle Assessment for the Design of Chemical Processes, Products, and Supply Chains <i>Johanna Kleinekorte, Lorenz Fleitmann, Marvin Bachmann, Arne Kätelhön, Ana Barbosa-Póvoa, Niklas von der Assen, and André Bardow</i>	203

Mechanistic Modeling of Preparative Column Chromatography for Biotherapeutics <i>Vijesh Kumar and Abraham M. Lenhoff</i>	235
Molecular Modeling and Simulations of Peptide–Polymer Conjugates <i>Phillip A. Taylor and Arthi Jayaraman</i>	257
Multiscale Lithium-Battery Modeling from Materials to Cells <i>Guanchen Li and Charles W. Monroe</i>	277
<i>N</i> -Glycosylation of IgG and IgG-Like Recombinant Therapeutic Proteins: Why Is It Important and How Can We Control It? <i>Natalia I. Majewska, Max L. Tejada, Michael J. Betenbaugh, and Nitin Agarwal</i>	311
Numerical Methods for the Solution of Population Balance Equations Coupled with Computational Fluid Dynamics <i>Mohsen Shiea, Antonio Buffo, Marco Vanni, and Daniele Marchisio</i>	339
Positron Emission Particle Tracking of Granular Flows <i>C.R.K. Windows-Yule, J.P.K. Seville, A. Ingram, and D.J. Parker</i>	367
Possibilities and Limits of Computational Fluid Dynamics–Discrete Element Method Simulations in Process Engineering: A Review of Recent Advancements and Future Trends <i>Paul Kieckhefen, Swantje Pietsch, Maksym Dosta, and Stefan Heinrich</i>	397
Process Control and Energy Efficiency <i>Jodie M. Simkoff, Fernando Lejarza, Morgan T. Kelley, Calvin Tsay, and Michael Baldea</i>	423
Quorum Sensing Communication: Molecularly Connecting Cells, Their Neighbors, and Even Devices <i>Sally Wang, Gregory F. Payne, and William E. Bentley</i>	447
Separation Processes to Provide Pure Enantiomers and Plant Ingredients <i>Heike Lorenz and Andreas Seidel-Morgenstern</i>	469
Unconventional Catalytic Approaches to Ammonia Synthesis <i>Patrick M. Barboun and Jason C. Hicks</i>	503
Water Structure and Properties at Hydrophilic and Hydrophobic Surfaces <i>Jacob Monroe, Mikayla Barry, Audra DeStefano, Pinar Aydogan Gokturk, Sally Jiao, Dennis Robinson-Brown, Thomas Webber, Ethan J. Crumlin, Songi Han, and M. Scott Shell</i>	523

Water Treatment: Are Membranes the Panacea?

*Matthew R. Landsman, Rabul Sujanani, Samuel H. Brodfuehrer,
Carolyn M. Cooper, Addison G. Darr, R. Justin Davis, Kyungtae Kim,
Soyoon Kum, Lauren K. Nalley, Sheik M. Nomaan, Cameron P. Oden,
Akhilesh Paspureddi, Kevin K. Reimund, Lewis Stetson Rowles III,
Seulkki Yeo, Desmond F. Lawler, Benny D. Freeman, and Lynn E. Katz 559*

Errata

An online log of corrections to *Annual Review of Chemical and Biomolecular Engineering* articles may be found at <http://www.annualreviews.org/errata/chembioeng>